



## Role of sulfur in hydrotreating catalysis over nickel phosphide

Xinping Duan<sup>a</sup>, Yang Teng<sup>a</sup>, Anjie Wang<sup>a,\*</sup>, Victor M. Kogan<sup>b</sup>, Xiang Li<sup>a</sup>, Yao Wang<sup>a</sup>

<sup>a</sup> Department of Catalytic Chemistry and Engineering, State Key Laboratory of Fine Chemicals, Dalian University of Technology, 158 Zhongshan Road, Dalian 116012, PR China

<sup>b</sup> The N.D. Zelinsky Institute of Organic Chemistry, Russian Academy of Sciences, 47 Leninsky Prospect, Moscow 119991, Russia

### ARTICLE INFO

#### Article history:

Received 22 September 2008

Revised 3 December 2008

Accepted 4 December 2008

Available online 23 December 2008

#### Keywords:

Hydrodesulfurization

Sulfur

H<sub>2</sub>S passivation

Hydrodenitrogenation

Hydrodeoxygenation

Nickel phosphide

MCM-41

### ABSTRACT

The effect of using a mixture of 10 mol% H<sub>2</sub>S and H<sub>2</sub> to passivate a Ni<sub>2</sub>P/MCM-41 catalyst was studied. It was found that H<sub>2</sub>S passivation was superior to conventional O<sub>2</sub> passivation because it gave a higher HDS activity and required no post re-reduction. Chemisorption of CO indicated that the passivation layer covered or replaced the surface active sites. Characterization of X-ray photoelectron spectroscopy revealed that the sulfur species on the surface of the H<sub>2</sub>S-passivated Ni<sub>2</sub>P/MCM-41 were polysulfide ligands rather than S<sup>2-</sup> or S<sub>2</sub><sup>2-</sup> and the sulfur species were partially oxidized. A treatment with NH<sub>3</sub> was also used, and it was found that N species were strongly bonded to the surface sites of Ni<sub>2</sub>P. Hydrodesulfurization and hydrodenitrogenation/hydrodeoxygenation were carried out in an alternating sequential manner to study the effect of surface sulfur on the catalytic activity of Ni<sub>2</sub>P/MCM-41. Sulfur analysis of the spent catalysts revealed that the HDS activity correlated with the sulfur content retained on Ni<sub>2</sub>P/MCM-41, indicating that sulfur is part of the active sites of the HDS reaction.

© 2008 Elsevier Inc. All rights reserved.

### 1. Introduction

The challenge of producing cleaner engine fuels from increasingly low quality petroleum feedstocks has stimulated the investigation and development of high-performance hydrotreating catalysts. An appealing approach to deep hydrodesulfurization (HDS) and hydrodenitrogenation (HDN) is the development of new catalytic active phases other than the conventional Mo- or W-based sulfides. Transition metal carbides, nitrides, and phosphides are promising candidates. Metal carbides, nitrides, and phosphides all show very high activity in both HDS and HDN, but the carbides and nitrides are unstable in the presence of H<sub>2</sub>S [1,2]. The deactivation results from the transformation of metal carbides and nitrides to sulfides under typical HDS conditions. In contrast to carbides and nitrides, metal phosphides are stable against H<sub>2</sub>S.

For this new series of phosphide hydrotreating catalysts, many researchers have reported that sulfur is incorporated in the metal phosphide catalysts during HDS reactions [3–5]. Based on the characterization of spent nickel phosphides, Oyama et al. [3,6,7] proposed that the surface active phase is a nickel phosphosulfide, but that this active phase is unlikely to be NiPS<sub>3</sub>. Loboué et al. prepared unsupported nickel phosphides by the decomposition of NiPS<sub>3</sub> [8], which was synthesized either by a solid-state reaction route or by a soft chemistry route. Both nickel phosphides exhibited much higher HDS activities than MoS<sub>2</sub>, and elemental analysis

revealed the presence of sulfur in the spent catalysts. On the theoretical side, Nelson et al. used density functional theory (DFT) to examine possible structures for the phosphosulfide overlayer on the Ni<sub>2</sub>P(001) surface resulting from H<sub>2</sub>S adsorption and dissociation, as well as the replacement of surface phosphorus by sulfur [9]. They concluded that 50% of the surface phosphorus in the Ni<sub>2</sub>P structure can be replaced by sulfur under hydrotreating reactions. All these results indicate that sulfur is involved in the HDS or HDN in a typical hydrotreating process. The incorporation of sulfur is reported to lead to improved HDS activity for Ni<sub>2</sub>P catalysts. But Bussell and co-workers reported recently that sulfur might block the active sites of cobalt phosphide [5].

In the preparation of metal phosphides, it is essential to passivate the obtained metal phosphides prior to exposure to air or moisture because they react vigorously with oxygen and water, leading to the formation of metal oxides. In a typical passivation, a low concentration of O<sub>2</sub> (0.5–1.0%) in inert gas is used to mildly oxidize the surface of the metal phosphides in order to form a protective layer, which prevents the bulk oxidation of the phosphides. Since the oxides are not catalytically active, the catalyst has to be reduced at elevated temperatures prior to the hydrotreating reaction. In the fields of optoelectronic devices and photovoltaics, sulfur passivation by (NH<sub>4</sub>)<sub>2</sub>S or H<sub>2</sub>S is used to improve the electronic properties of III–V semiconductors, such as InP and GaP [10]. However, this passivation method has not been used in the preparation of phosphide catalysts.

In the present study, we employed the sulfur passivation using H<sub>2</sub>S in H<sub>2</sub> following the preparation of Ni<sub>2</sub>P, and investigated the relationship between the sulfur on Ni<sub>2</sub>P and the catalytic per-

\* Corresponding author. Fax: +86 411 39893693.

E-mail address: ajwang@chem.dlut.edu.cn (A. Wang).

formance in the HDS of dibenzothiophene (DBT), in the HDN of quinoline, and in the hydrodeoxygenation (HDO) of phenol.

## 2. Experimental

### 2.1. Preparation of unsupported and supported Ni<sub>2</sub>P

Unsupported nickel phosphide (Ni<sub>2</sub>P) was prepared from an oxidic precursor with Ni/P atomic ratio of 1.25. An amount of 1.6 g (NH<sub>4</sub>)<sub>2</sub>HPO<sub>4</sub> was dissolved in 10 mL of deionized water to form a transparent colorless solution, then 4.4 g Ni(NO<sub>3</sub>)<sub>2</sub>·6H<sub>2</sub>O was added. The clear solution immediately became cloudy but, when the pH of the mixture was adjusted to 2–3 using 0.5 M HNO<sub>3</sub>, it became clear again. The water was then evaporated and the resulting solid was dried at 120 °C overnight, followed by calcination in air at 500 °C for 3 h. The obtained oxidic precursor was then pelleted, crushed, and sieved to 20–35 mesh.

Mesoporous MCM-41 was synthesized according to a procedure described before [11]. The synthesized siliceous MCM-41 had a specific surface area of 1028 m<sup>2</sup> g<sup>-1</sup>, a pore volume of 0.90 cm<sup>3</sup> g<sup>-1</sup>, and a BJH average pore size of 3.4 nm. The siliceous MCM-41-supported Ni<sub>2</sub>P was prepared from an oxidic precursor with a total loading of 30 wt% NiO and P<sub>2</sub>O<sub>5</sub> (Ni/P = 1.25). An aqueous solution of 2.07 g of (NH<sub>4</sub>)<sub>2</sub>HPO<sub>4</sub> and 5.69 g Ni(NO<sub>3</sub>)<sub>2</sub>·6H<sub>2</sub>O in 20 mL of deionized water was prepared according to the procedure mentioned above. A quantity of 6.00 g of MCM-41 was evacuated for 0.5 h and then wet-impregnated with the prepared solution for 0.5 h at room temperature. The mixture was heated to evaporate the water, and then the obtained solid was dried at 120 °C overnight, followed by calcination in air at 500 °C for 3 h. The oxidic precursor was pelleted, crushed, and sieved to 20–35 mesh.

The unsupported or supported oxidic precursor was subjected to a temperature-programmed hydrogen reduction in a U-shaped tubular reactor. The temperature program included two stages: (1) heating at 5 °C min<sup>-1</sup> from room temperature to 120 °C and maintaining at 120 °C for 1 h to remove adsorbed moisture in a H<sub>2</sub> flow (150 mL min<sup>-1</sup>); (2) further heating from 120 to 400 °C at 5 °C min<sup>-1</sup> and from 400 to 550 °C at 1 °C min<sup>-1</sup>, then holding the temperature at 550 °C for 3 h.

To protect the metal phosphide structures, it is essential to passivate them before they are exposed to air. In the conventional method [12–14], the prepared Ni<sub>2</sub>P is passivated in a 1.0 mol% O<sub>2</sub>/He flow (30 mL min<sup>-1</sup>) at ambient temperature and pressure for 2 h. Here, we used 10 mol% H<sub>2</sub>S/H<sub>2</sub> to replace the 1.0 mol% O<sub>2</sub>/He in the passivation at otherwise similar conditions. For comparison, we also tried treatment with gaseous NH<sub>3</sub> for 1 h.

### 2.2. Hydrotreating reaction

The HDS, HDN, and HDO reactions were carried out in a tubular stainless steel trickle-bed reactor [15]. For a typical reaction, a charge of 0.2 g of the passivated Ni<sub>2</sub>P catalyst was used, and held in the middle of the reactor by two layers of quartz sand. Prior to reaction, the catalyst was reduced at 500 °C for 1 h in a H<sub>2</sub> flow (150 mL min<sup>-1</sup>). For comparison, MCM-41-supported Ni<sub>2</sub>P was prepared by an *in situ* reduction method in the same reactor [15]. For the *in situ* prepared and H<sub>2</sub>S-passivated catalysts, a reduction at elevated temperature was not needed. The HDS activity of the catalyst was evaluated using 0.8 wt% DBT in decalin, the HDN performance was measured using 1 wt% quinoline in decalin, and the HDO activity was tested using 1 wt% phenol in decalin. The conditions for the HDS, HDN, and HDO reactions were 300 °C, 4 MPa, WHSV = 24 h<sup>-1</sup>, and a H<sub>2</sub> flow rate of 50 mL min<sup>-1</sup>. The sampling of liquid products was started 3 h after start of the reaction when conditions had stabilized, and liquid samples were collected at 1 h

intervals. Both feed and liquid samples were analyzed by means of an Agilent-6890<sup>+</sup> gas chromatograph equipped with an FID detector using a commercial HP-5 capillary column (5% phenyl methyl polysiloxane, 30.0 m × 320 μm × 0.25 μm).

In the HDS of DBT, only small amounts of sulfur-containing intermediates were detected and therefore we used the conversion of DBT to measure the HDS performance of the catalysts. Sulfur removal in the HDS of DBT follows two pathways: (1) the direct desulfurization (DDS) pathway, in which sulfur atom is removed by S–C bond cleavage to form biphenyl (BP); (2) the hydrogenation (HYD) pathway, in which one of the aromatic rings is first hydrogenated and then the sulfur atom is removed. Because biphenyl is hardly hydrogenated to cyclohexyl benzene in the presence of sulfur species, the BP selectivity (*S*<sub>BP</sub>) is used as a measure of the DDS pathway activity, and (1 – *S*<sub>BP</sub>) to represent the HYD pathway activity.

In the HDN of quinoline, the conversion of quinoline is high, but most products are nitrogen-containing tetrahydroquinoline intermediates. Therefore we define the HDN conversion as

$$\text{HDN conversion} = \frac{C_{Q0} - C_{QR} - C_{NC}}{C_{Q0}} \times 100, \quad (1)$$

where *C*<sub>Q0</sub> represents the quinoline concentration in the feed, *C*<sub>QR</sub> is the quinoline concentration in the HDN liquid product, and *C*<sub>NC</sub> describes the sum of the concentrations of all the nitrogen-containing intermediates in the HDN liquid product. The conversion of phenol is used to represent the HDO performance.

To investigate the effect of the sulfur retained on the Ni<sub>2</sub>P catalyst in the hydrotreating reactions, we conducted the HDS and HDN (HDO) in an alternating sequence. After the reaction, the catalyst was flushed with cyclohexane and N<sub>2</sub> at 300 °C for 2 h to remove the physically absorbed sulfur species. Then the spent catalyst was transferred to the sulfur measurement unit. The total amount of sulfur in the catalyst was determined using a high-temperature combustion method according to the ASTM D 4239–05 procedure. Briefly, a weighed sample was burned in a tube furnace at 1000 °C in a stream of oxygen. During combustion, all sulfur species contained in the sample are oxidized to gaseous oxides of sulfur (SO<sub>2</sub> and SO<sub>3</sub>). The gaseous products were then absorbed into a solution of H<sub>2</sub>O<sub>2</sub>, forming a dilute solution of H<sub>2</sub>SO<sub>4</sub>. The sulfur content of the sample was calculated from the acid quantity determined by titration. The nitrogen contents of spent catalysts were measured on a Vario EL elemental analyzer.

### 2.3. Characterization

Powder X-ray diffraction (XRD) measurements were performed on a Rigaku D/max-2400 instrument using CuKα radiation (λ = 1.54 Å) and a scan rate of 5° min<sup>-1</sup>, at 40 kV and 100 mA.

Fourier transform infrared (FTIR) spectra of pyridine adsorbed on the passivated Ni<sub>2</sub>P/MCM-41 were recorded using an Equinox 55 instrument. Rectangular self-supported wafers of the samples were prepared from the catalyst powder and placed in the sample holder in an IR cell. After evacuation for 2 h, background spectra were measured, and then the samples were exposed to pyridine at room temperature for 10 min. The wafers containing chemisorbed pyridine were subjected to thermal treatment at 100 °C in vacuum and cooled to room temperature, and then the IR spectra were measured again.

To investigate the relationship between passivation and active sites, the CO adsorption capacity of the catalysts was measured without re-reduction using a Chembet 3000 analyzer. Pulses of 1% CO in Ar were injected until breakthrough. The CO uptake of the sample was calculated from the accumulated difference in the peak areas of input and output signals.

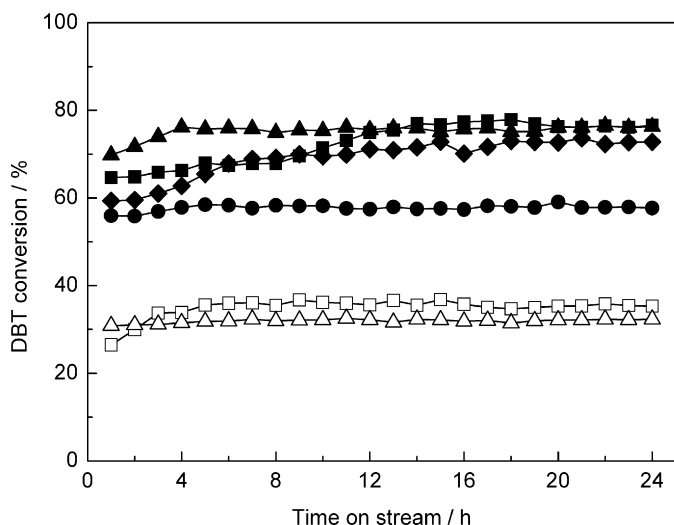


**Fig. 1.** Variation of DBT conversion in HDS catalyzed by  $Ni_2P/MCM-41$  catalysts post-treated by different methods: ( $\blacksquare$ ) *in situ* reduction, ( $\blacktriangle$ )  $H_2S$  passivation, ( $\bullet$ )  $O_2$  passivation, ( $\blacklozenge$ )  $O_2$  passivation and  $H_2$  reduction, ( $\triangle$ )  $NH_3$  passivation, ( $\square$ )  $NH_3$  passivation and  $H_2$  reduction.

Transmission electron microscope (TEM) images were acquired using a JEOL 2010 high-resolution TEM operating at 200 kV. Samples of the unsupported  $Ni_2P$  catalysts were placed on a 200-mesh copper grid coated with formvar and carbon.

X-ray photoelectron spectroscopy (XPS) spectra of the  $O_2$ -,  $H_2S$ -, and  $NH_3$ -passivated  $Ni_2P/MCM-41$  catalysts were acquired with a Multilab2000 X-ray photoelectron spectrometer, using a  $MgK\alpha$  source. For the individual energy regions, a pass energy of 20 eV was used. All binding energies were referenced to the C 1s peak at 284.6 eV.

To clarify the adsorption or bonding of sulfur or nitrogen on  $Ni_2P$  after passivation, temperature-programmed desorption (TPD) was conducted in He. The  $NH_3$ - and  $H_2S$ -passivated samples were prepared in the TPD apparatus, and were not exposed to air. The spent catalyst was not pretreated prior to TPD measurement. The TPD profiles were measured on a Chembet 3000 analyzer, using 0.2 g of sample heated in a He flow ( $40\text{ mL min}^{-1}$ ) at  $10^\circ\text{C min}^{-1}$  up to  $900^\circ\text{C}$ .

### 3. Results

#### 3.1. Passivation by $H_2S$

Like with metal nitrides and carbides, when a metal phosphide is exposed to air, it will be oxidized violently to its oxide. Therefore, a passivation procedure, conventionally mild oxidation by low concentration  $O_2$  in Ar, He, or  $N_2$ , is essential when exposure of the metal phosphide to air is inevitable.

In the present study, we investigated the use of 10%  $H_2S$  in  $H_2$  to passivate freshly prepared  $Ni_2P$  at ambient temperature and pressure. The HDS performance of the  $H_2S$ -passivated  $Ni_2P/MCM-41$  at  $300^\circ\text{C}$  and 4.0 MPa is shown in Fig. 1, together with those of  $Ni_2P/MCM-41$  catalysts prepared by *in situ* reduction, conventional  $O_2$  passivation– $H_2$  reduction ( $500^\circ\text{C}$  for 1 h),  $O_2$  passivation without  $H_2$  reduction,  $NH_3$  passivation– $H_2$  reduction ( $500^\circ\text{C}$  for 1 h), and  $NH_3$  passivation without  $H_2$  reduction. It is clear that  $H_2$  reduction at  $500^\circ\text{C}$  is essential to achieve high performance for the  $O_2$ -passivated  $Ni_2P/MCM-41$ . After  $H_2$  reduction, the  $O_2$ -passivated  $Ni_2P/MCM-41$  showed a slightly higher HDS activity than the unreduced  $Ni_2P/MCM-41$  in the first 2 h. Thereafter, the HDS activity of the reduced  $Ni_2P/MCM-41$  increased gradually with reaction time until a steady conversion of DBT was achieved after

15 h, suggesting that a surface reconstruction takes place during the HDS reaction. Without  $H_2$  reduction prior to HDS reaction, the  $O_2$ -passivated  $Ni_2P/MCM-41$  showed a lower but stable HDS activity. This lower activity suggests that  $O_2$  passivation irreversibly destroys part of the surface structure of  $Ni_2P$ .

The  $H_2S$ -passivated  $Ni_2P/MCM-41$  showed comparable HDS performance to the  $Ni_2P/MCM-41$  prepared by the *in situ* reduction method in steady state. The HDS activity of the  $H_2S$ -passivated  $Ni_2P/MCM-41$  reached the steady state in 4 h, suggesting that slight surface reconstruction takes place during HDS reaction. In contrast, it took much longer for the *in situ* prepared  $Ni_2P/MCM-41$  to achieve the steady state. The HDS reaction may be involved in the reconstruction of the surface. Both the  $H_2S$ -passivated  $Ni_2P/MCM-41$  and the *in situ* prepared  $Ni_2P/MCM-41$  (TOF  $0.012\text{ s}^{-1}$  at steady state) showed higher HDS activities than the  $O_2$ -passivated  $Ni_2P/MCM-41$ , even the one re-reduced at  $500^\circ\text{C}$ . For the *in situ* prepared  $Ni_2P/MCM-41$ , the phosphide was not exposed to air, avoiding damage of the surface. The comparable HDS performance of the  $H_2S$ -passivated  $Ni_2P/MCM-41$  to that of the *in situ* prepared  $Ni_2P/MCM-41$  suggests that  $H_2S$  passivation is an effective way to protect the surface structure of nickel phosphide.

In addition to  $O_2$  and  $H_2S$ , we also investigated gaseous  $NH_3$  to passivate  $Ni_2P/MCM-41$ , taking into consideration that nitrogen species are involved in hydrotreating catalysis as well.  $NH_3$  passivation gave much lower HDS activity than  $O_2$  or  $H_2S$  passivation (Fig. 1). In contrast to  $O_2$  passivation, only slight improvement was observed after  $H_2$  reduction at  $500^\circ\text{C}$  for 1 h.

The DDS and HYD selectivities (Fig. 2) indicated that the HDS of DBT occurred mainly by the DDS pathway. Moreover, the pathway selectivity was about equal for all the catalysts, implying that the post treatment does not remarkably affect the nature of the active phase but only the number of active sites on the surface of the catalysts.

Fig. 3 shows the XRD patterns of  $Ni_2P/MCM-41$  passivated by  $O_2$ ,  $H_2S$ , and  $NH_3$ . The patterns were not affected by the various passivations, indicating that  $O_2$ ,  $H_2S$ , and  $NH_3$  might be bonded to the surface of  $Ni_2P$  in the passivations so as to suppress further vigorous oxidation.

CO chemisorption can be used as a measure of active sites on metal phosphide catalysts [3]. For  $Ni_2P/MCM-41$  without exposure to air, the CO uptake was  $15\text{ }\mu\text{mol g}^{-1}$ . When the catalyst was passivated using  $O_2$ ,  $H_2S$ , or  $NH_3$ , the CO uptake became undetectable, suggesting that all passivating reagents were strongly bonded to the surface active sites, in addition to leading to the formation of protection layers.

TEM images of the  $O_2$ - and  $H_2S$ -passivated bulk  $Ni_2P$  particles (Fig. 4) were taken to investigate any changes on the surface layers. In each sample, the crystal particles were surrounded by an amorphous layer of 1–3 nm. Both passivation procedures gave rise to surface reconstruction of the crystalline  $Ni_2P$  particles. On the average, the  $H_2S$ -passivated  $Ni_2P$  particle had a smooth external surface whereas the  $O_2$ -passivated one had a rough surface or burl-shaped particles, indicating that more severe reconstruction took place in  $O_2$  passivation than in  $H_2S$  passivation.

For each passivation method, the stability of the resulting passivated nickel phosphide is of great importance. To investigate the stability of the passivated  $Ni_2P/MCM-41$ , we compared the HDS performance of a freshly passivated catalyst with that of samples which were kept in air for 30 and 150 days after the  $H_2S$  passivation. Fig. 5 indicates that the  $H_2S$ -passivated  $Ni_2P/MCM-41$  was stable in air for 30 days. After 150 days storage in air, the catalyst showed lower HDS activity in the first few hours, but its activity resumed at steady state.

Fig. 6 shows the TPD profiles of  $H_2S$ -passivated  $Ni_2P/MCM-41$ , spent  $Ni_2P/MCM-41$ , and  $NH_3$ -passivated  $Ni_2P/MCM-41$  in a flow

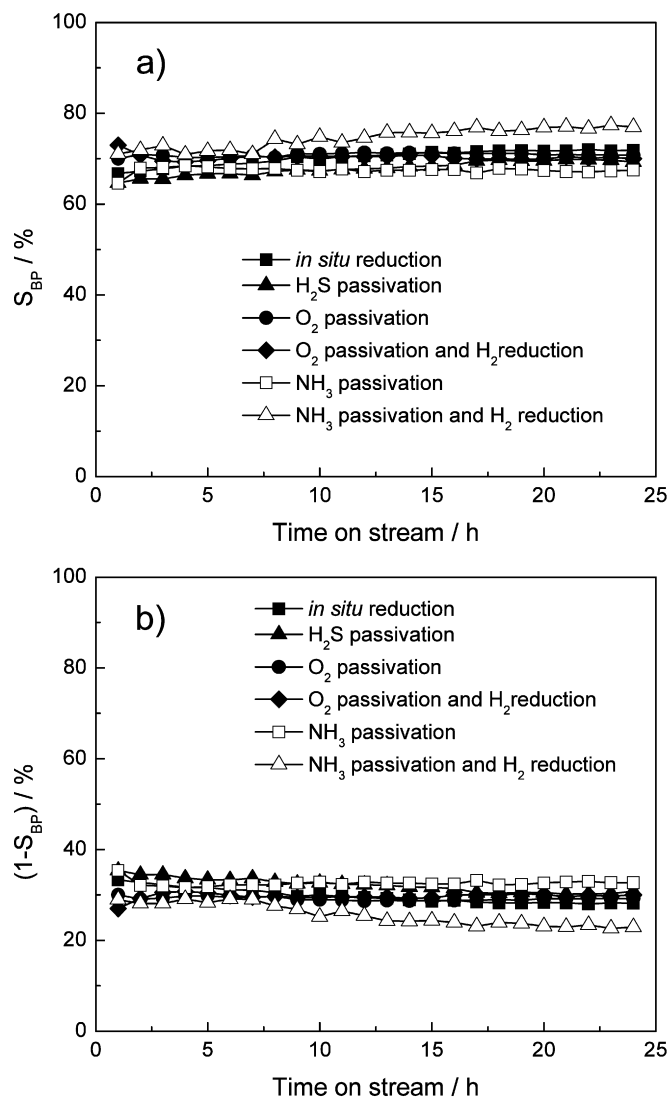


**Fig. 2.** Selectivities of DDS and HYD pathways in the HDS of DBT catalyzed by  $\text{Ni}_2\text{P}/\text{MCM-41}$  catalysts post-treated by different methods: (■) *in situ* reduction, (▲)  $\text{H}_2\text{S}$  passivation, (●)  $\text{O}_2$  passivation, (◆)  $\text{O}_2$  passivation and  $\text{H}_2$  reduction, (□)  $\text{NH}_3$  passivation, (△)  $\text{NH}_3$  passivation and  $\text{H}_2$  reduction.

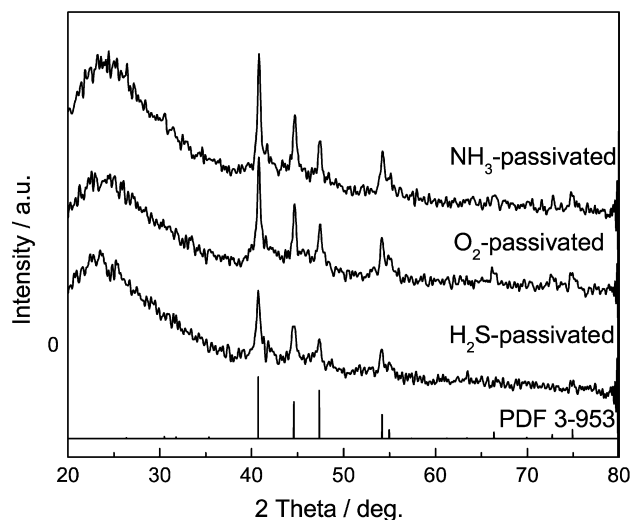


**Fig. 3.** XRD patterns of  $\text{Ni}_2\text{P}/\text{MCM-41}$  passivated by different methods.

of He at a heating rate of  $10^\circ\text{Cmin}^{-1}$ . There are two groups of desorption peaks in the TPD curve of the spent catalyst and only one group in that of the  $\text{H}_2\text{S}$ -passivated  $\text{Ni}_2\text{P}/\text{MCM-41}$ . The group at low temperature might correspond to adsorbed  $\text{H}_2\text{S}$  and  $-\text{SH}$  groups on the surface of  $\text{Ni}_2\text{P}$ . The group in the high temperature range might be ascribed to the cleavage of strong chemical bonds between sulfur and nickel and/or phosphorus, or to the decomposition of sulfur species in the subsurface of the  $\text{Ni}_2\text{P}$  crystal.  $\text{H}_2\text{S}$  passivation might give rise to weak coordination of sulfur with the surface sites of  $\text{Ni}_2\text{P}$ , but structural reconstruction of the surface and subsurface might continue to take place in the course of HDS. The broad peak and its shoulder in the TPD curve of the  $\text{NH}_3$ -passivated  $\text{Ni}_2\text{P}/\text{MCM-41}$  in the high temperature range indicate that  $\text{NH}_3$  has stronger interaction with the active sites than  $\text{H}_2\text{S}$ .

The surface acidity of the samples was determined by FTIR spectroscopy of adsorbed pyridine. The FTIR spectra of pyridine-adsorbed  $\text{Ni}_2\text{P}/\text{MCM-41}$  passivated by different gases are shown in Fig. 7. Three main absorption bands around 1450, 1490, and  $1610\text{ cm}^{-1}$  were observed for all the passivated samples. According to the literature, the bands at 1610 and  $1450\text{ cm}^{-1}$  correspond to vibrations of pyridine adsorbed on Lewis acid sites whereas the band at  $1490\text{ cm}^{-1}$  is assigned to the contributions of both the Lewis acid and Brønsted acid sites to pyridine adsorption. The spectra show that Lewis acidity is predominant in  $\text{Ni}_2\text{P}/\text{MCM-41}$ . Our previous study showed that few Lewis acid sites are present on siliceous MCM-41 [16]. Therefore,  $\text{Ni}_2\text{P}$  might contribute to the Lewis acidity of the catalysts. The adsorption bands at 1643 and  $1548\text{ cm}^{-1}$  indicate the presence of Brønsted acid sites on the  $\text{H}_2\text{S}$ -passivated  $\text{Ni}_2\text{P}/\text{MCM-41}$ . The Brønsted acid sites might be related to the  $-\text{SH}$  groups or the adsorbed  $\text{H}_2\text{S}$  on the surface [17]. The very weak adsorption bands at 1643 and  $1548\text{ cm}^{-1}$  in the spectrum of  $\text{O}_2$ -passivated  $\text{Ni}_2\text{P}/\text{MCM-41}$  might result from the interaction of pyridine with P-OH groups in the surface layer [18]. There is no distinct adsorption band at 1643 or  $1548\text{ cm}^{-1}$  in the spectrum of  $\text{NH}_3$ -passivated  $\text{Ni}_2\text{P}/\text{MCM-41}$ , probably due to the basic nature of  $\text{NH}_3$ .

The XPS spectra in the Ni(2p), P(2p), S(2p) and N(1s) regions for  $\text{Ni}_2\text{P}/\text{MCM-41}$  catalysts passivated by  $\text{O}_2$ ,  $\text{H}_2\text{S}$ , and  $\text{NH}_3$  are shown in Fig. 8. For the  $\text{O}_2$ -passivated  $\text{Ni}_2\text{P}/\text{MCM-41}$ , the peaks at 857.4 (Fig. 8a) and 134.2 eV (Fig. 8b) in the Ni(2p) and P(2p) regions are assigned to  $\text{Ni}^{2+}$  and  $\text{P}^{5+}$  species, respectively, in the passivated layer formed on the surface of  $\text{Ni}_2\text{P}$  particles [13,19]. The peak observed at 853.6 eV (Fig. 8a) is assigned to reduced Ni. The peak ascribed to reduced P species at 129.0 eV (Fig. 8b) [13,19] was hardly observed, probably due to the low resolution of the XPS analyzer. Compared with the  $\text{O}_2$ -passivated  $\text{Ni}_2\text{P}/\text{MCM-41}$ , negative shifts of binding energies of surface  $\text{Ni}^{2+}$  species (shifted from 857.4 to 856.6 eV), the reduced Ni species (shifted from 853.6 to 853.3 eV) and  $\text{P}^{5+}$  species (shifted from 134.2 to 133.5 eV) were observed for  $\text{NH}_3$ -passivated  $\text{Ni}_2\text{P}/\text{MCM-41}$ . Nevertheless, no significant differences in XPS spectra of  $\text{O}_2$ - and  $\text{H}_2\text{S}$ -passivated  $\text{Ni}_2\text{P}/\text{MCM-41}$  were observed. The binding energies of  $\text{Ni}^{2+}$  and  $\text{P}^{5+}$  species in  $\text{H}_2\text{S}$ -passivated  $\text{Ni}_2\text{P}/\text{MCM-41}$  were only 0.3 eV lower than those in  $\text{O}_2$ -passivated  $\text{Ni}_2\text{P}/\text{MCM-41}$ , and the binding energies of the reduced Ni species in the two samples were essentially the same. Fig. 8c only shows the S(2p) spectrum of  $\text{H}_2\text{S}$ -passivated  $\text{Ni}_2\text{P}/\text{MCM-41}$  because no signal was detected for the other two samples in this region. The S(2p) features exhibited two distinct peaks. The 163.7 eV peak was assigned to the polysulfide ligands ( $\text{S}_n^{2-}$ ) [20,21], whereas the 169.7 peak revealed the presence of highly oxidized surface sulfate species or sulfonic species [20,21]. On the other hand, only one peak at 399.9 eV was detected in the N(1s) spectrum of the  $\text{NH}_3$ -passivated  $\text{Ni}_2\text{P}/\text{MCM-41}$  (Fig. 8d).

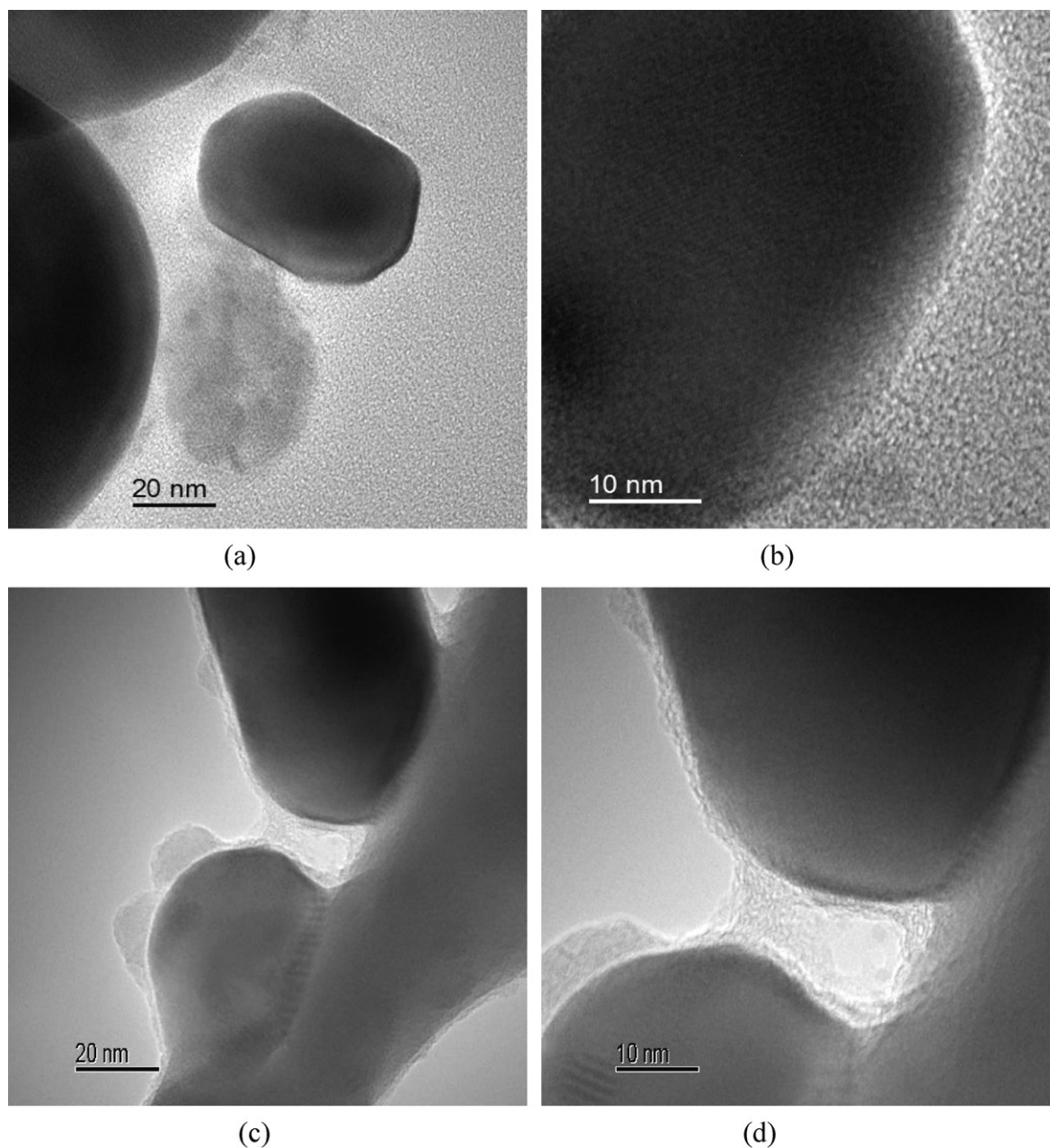


Fig. 4. TEM images of H<sub>2</sub>S-passivated Ni<sub>2</sub>P particle (a, b) and O<sub>2</sub>-passivated one (c, d).

### 3.2. Role of sulfur in HDS, HDN, and HDO

To investigate the effects of sulfur, nitrogen, and oxygen on the catalytic performance of H<sub>2</sub>S-passivated Ni<sub>2</sub>P/MCM-41, we conducted alternating measurement of HDS and HDN or HDO activity. Fig. 9 shows the variation of the HDS or HDN activity of H<sub>2</sub>S-passivated Ni<sub>2</sub>P/MCM-41 with reaction time in the course of HDS–HDN–HDS. The HDS reaction started with 0.8 wt% DBT in decalin at 300 °C, 4.0 MPa, and WHSV 24 h<sup>-1</sup>. In a few hours, the HDS activity reached steady state. After 24 h of HDS reaction, the feed was switched to 1.0 wt% quinoline in decalin, while keeping the same temperature, pressure, and WHSV. The HDN activity was much lower than the HDS activity, but was stable. When the feed was switched back to the decalin solution of 0.8 wt% DBT, the HDS activity was initially much lower than that in the first HDS run. The HDS activity increased gradually, but did not recover completely in 48 h.

On the other hand, if we started with HDN instead of HDS, the HDN activity was higher than that of HDN after HDS (Fig. 10). However, the catalyst showed much lower activity in the subsequent HDS, and the recovery of the HDS activity was again very slow.

When we replaced the HDN by the HDO of phenol, the results were quite different. As shown in Fig. 11, when the feed was switched from DBT to phenol, the HDO activity increased gradually until complete conversion of phenol was reached. The catalyst showed a dramatically high HDO activity and was stable up to 100 h. When the feed was switched back to DBT, the HDS performance resumed immediately, but the HDS activity was lower than in the first run.

Table 1 summarizes the sulfur and nitrogen contents of Ni<sub>2</sub>P/MCM-41 after H<sub>2</sub>S passivation as well as after HDS, HDN, and HDO. After H<sub>2</sub>S passivation, 0.66 wt% sulfur (206 μmol g<sup>-1</sup>) was absorbed or incorporated on the surface of Ni<sub>2</sub>P/MCM-41 (entry 1),

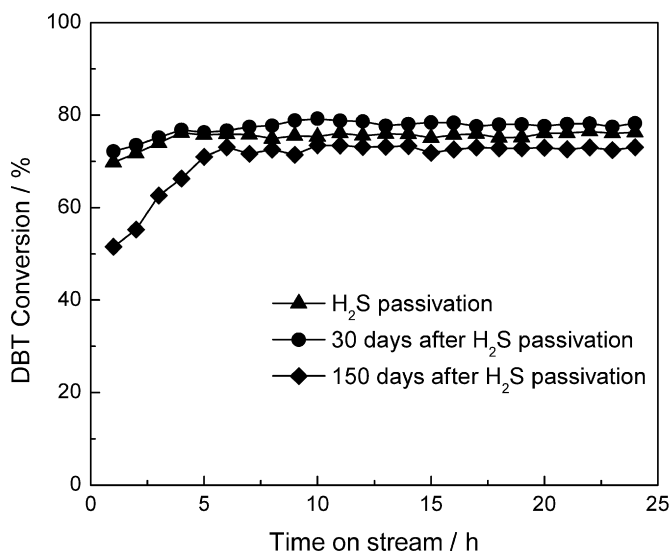


Fig. 5. Stability of the H<sub>2</sub>S-passivated Ni<sub>2</sub>P/MCM-41.

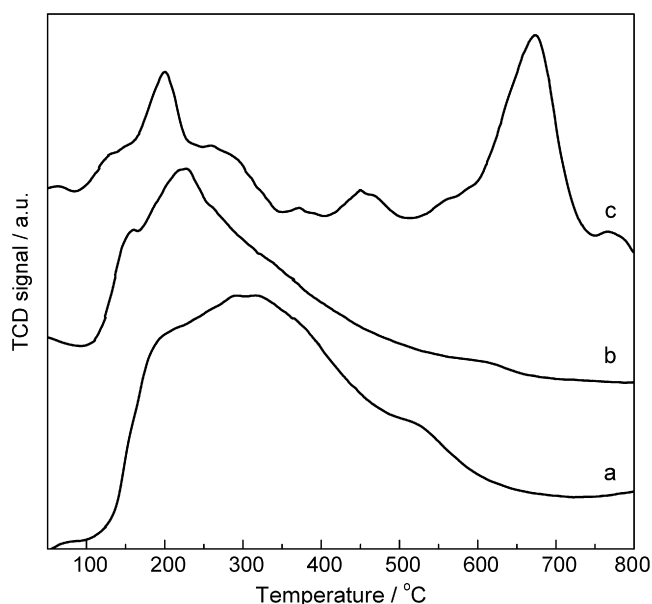


Fig. 6. Temperature-programmed desorption profiles of the NH<sub>3</sub>-passivated (a), H<sub>2</sub>S-passivated (b), and spent (c) Ni<sub>2</sub>P/MCM-41 catalysts in He.

which was comparable to that of the *in situ* prepared Ni<sub>2</sub>P/MCM-41 after 24 h of HDS reaction (entry 2). Comparing with the CO uptake ( $15 \mu\text{mol g}^{-1}$ ) with the sulfur retained on the passivated surface, one may conclude that, in addition to covering the active sites, the sulfur species might be mainly adsorbed on or incorporated into the passivation layer. After HDS reaction, the sulfur contents changed slightly for the H<sub>2</sub>S-passivated Ni<sub>2</sub>P/MCM-41, either fresh or after exposure in air for 30 d (entries 3 and 4). The sulfur contents of the O<sub>2</sub>- and NH<sub>3</sub>-passivated Ni<sub>2</sub>P/MCM-41 (entries 6 and 7) were much lower than that of the H<sub>2</sub>S-passivated catalyst after 24 h of HDS reaction (entry 3). Moreover, the sulfur content of the O<sub>2</sub>-passivated and H<sub>2</sub>-reduced Ni<sub>2</sub>P/MCM-41 (entry 5) was slightly lower than that of the H<sub>2</sub>S-passivated one. The sulfur content of the H<sub>2</sub>S-passivated Ni<sub>2</sub>P/MCM-41 after HDS-HDO (entry 9) was equal to that after HDS-HDN (entry 10), suggesting that oxygen and nitrogen might have replaced the same kind of sulfur species on the catalyst. When they were subjected to HDS again, the sulfur contents on both catalysts increased remarkably (entries 11 and 12), accompanied by the increase of HDS activ-

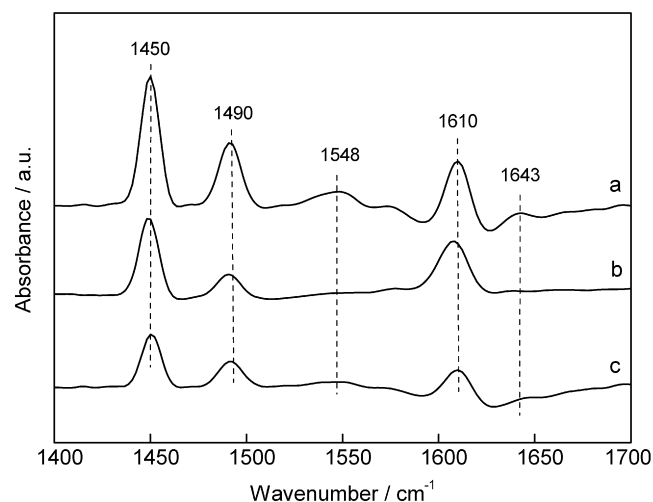


Fig. 7. FT-IR spectra of pyridine absorbed on Ni<sub>2</sub>P/MCM-41 passivated by H<sub>2</sub>S (a), NH<sub>3</sub> (b), and O<sub>2</sub> (c).

ity. However, if the reaction started with HDN catalyzed by H<sub>2</sub>S-passivated Ni<sub>2</sub>P/MCM-41, the sulfur content changed only little after subsequent HDS (entries 13 and 14), indicating the difficulty of replacing nitrogen species by sulfur species. It is important to note that the total contents of sulfur and nitrogen of the spent Ni<sub>2</sub>P/MCM-41 catalysts, over which HDN had taken place for over 24 h, were equivalent, suggesting the exchange between sulfur and nitrogen species in switching between HDS and HDN.

To correlate the HDS performance with the sulfur content of Ni<sub>2</sub>P/MCM-41 after HDS reaction, we plotted the DBT conversion against sulfur content of various Ni<sub>2</sub>P/MCM-41 catalysts after HDS reaction (Fig. 12). The HDS performance correlates well with the sulfur content of the catalyst after HDS reaction except for NH<sub>3</sub>-passivated Ni<sub>2</sub>P/MCM-41, suggesting that sulfur acts as part of the catalytic centers for the HDS reaction.

#### 4. Discussion

Metal phosphides will be damaged when they are exposed to air, due to a vigorous oxidation or even burning in the presence of high-concentration oxygen. To avoid structural damage, a passivation process must be used when transferring the phosphide catalyst from a preparation unit to a reactor. Because the oxides are not catalytically active, a decrease in HDS activity is observed if the O<sub>2</sub>-passivated catalyst has not been reduced at elevated temperatures (i.e. 500 °C), prior to HDS reaction (Fig. 1). The Ni<sub>2</sub>P/MCM-41 prepared by *in situ* reduction showed higher HDS activity than the one prepared by the conventional reduction-passivation-reduction method, implying that the nickel phosphide structure could not be completely recovered by H<sub>2</sub> reduction of the O<sub>2</sub>-passivated Ni<sub>2</sub>P/MCM-41.

According to DFT calculations [9], Nelson et al. found that the surface of Ni<sub>2</sub>P is not energetically homogeneous. Structures with sulfur on the surface are more stable than a clean Ni<sub>2</sub>P surface with free H<sub>2</sub>S molecules in the gas phase. The relative stability at low temperature increases in the order: (free H<sub>2</sub>S + Ni<sub>2</sub>P clean surface) < (H<sub>2</sub>S adsorbed on Ni<sub>2</sub>P surface) < (adsorbed -SH + one-half free hydrogen molecule) < (adsorbed sulfur atom + free hydrogen molecule). H<sub>2</sub>S is prone to dissociate on the surface of Ni<sub>2</sub>P at low temperature and replace the phosphorus atoms at high energy levels on the surface. This suggests that H<sub>2</sub>S might be an alternative passivating reagent in the preparation of nickel phosphide catalysts.

The H<sub>2</sub>S-passivated Ni<sub>2</sub>P/MCM-41 exhibited a higher HDS activity than the O<sub>2</sub>-passivated one (Fig. 1). Re-reduction at 500 °C by

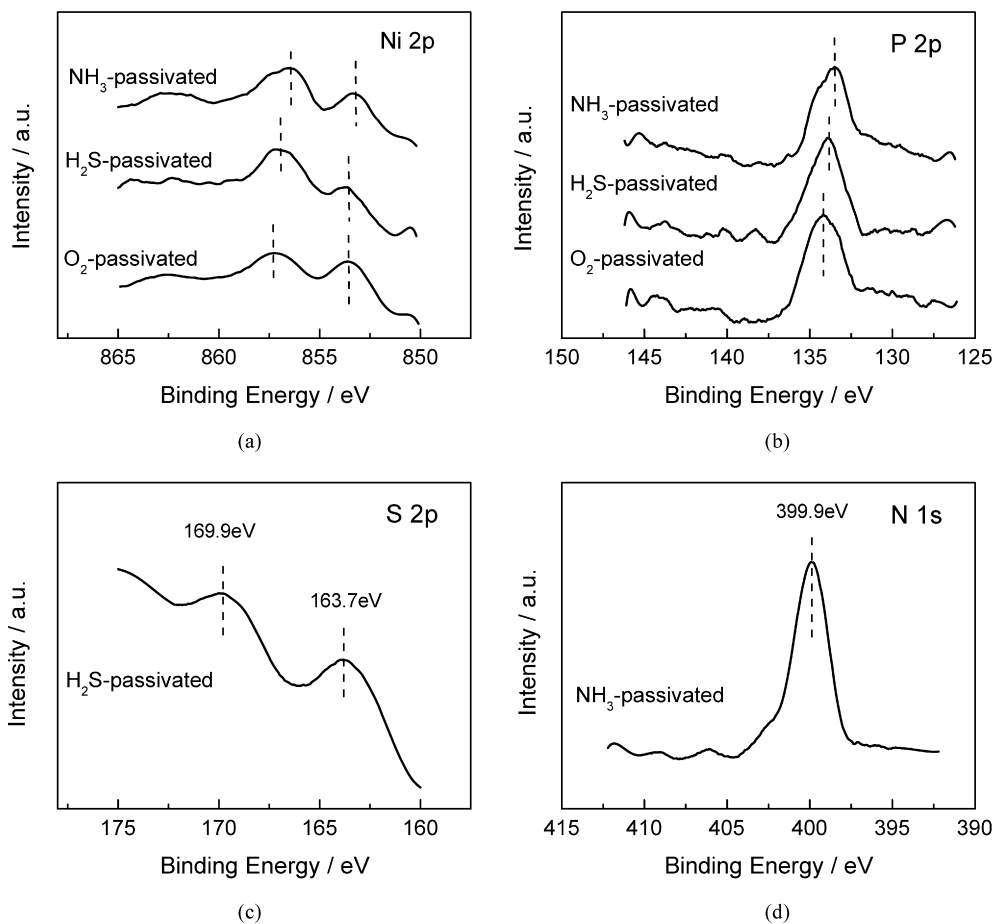


Fig. 8. XPS spectra of  $\text{Ni}_2\text{P}/\text{MCM-41}$  catalysts passivated by different methods.

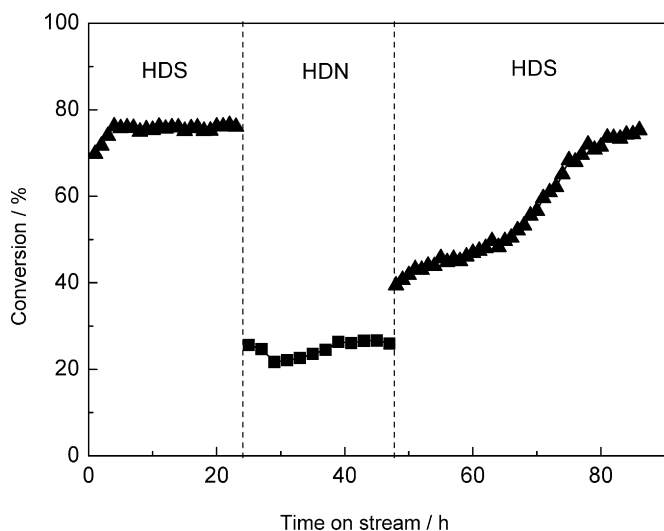


Fig. 9. Performance of  $\text{H}_2\text{S}$ -passivated  $\text{Ni}_2\text{P}/\text{MCM-41}$  in the consecutive HDS, HDN, and HDS.

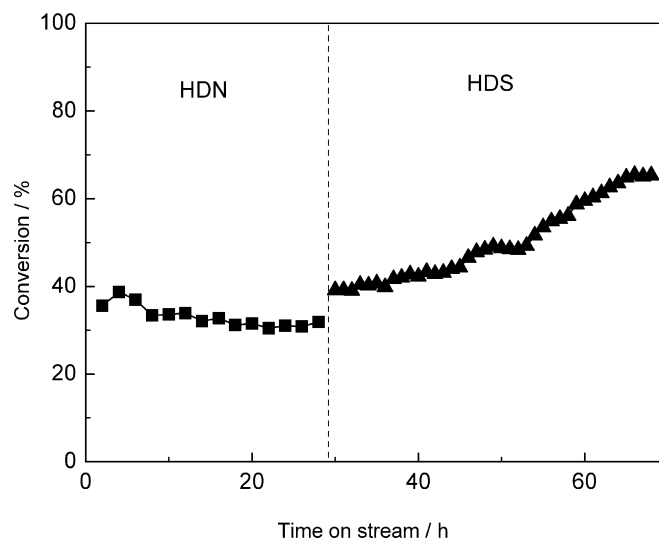
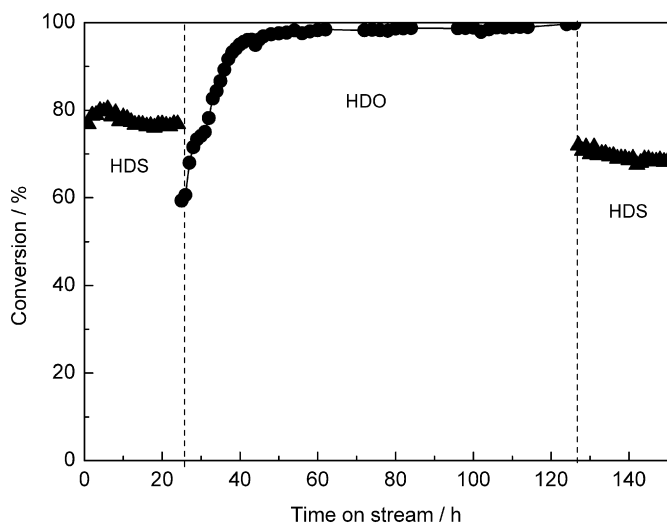


Fig. 10. Performance of  $\text{H}_2\text{S}$ -passivated  $\text{Ni}_2\text{P}/\text{MCM-41}$  in the HDN of quinoline and in the consecutive HDS of DBT.

hydrogen improved the performance of the  $\text{O}_2$ -passivated catalyst, but the resulting HDS activity was not as high as that of the  $\text{H}_2\text{S}$ -passivated catalyst. This is in agreement with a result reported by Sawhill et al. [13]. They found that an  $\text{O}_2$ -passivated  $\text{Ni}_2\text{P}/\text{SiO}_2$  catalyst showed a higher HDS activity when it was subjected to sulfidation by  $\text{H}_2\text{S}/\text{H}_2$  than to  $\text{H}_2$  reduction. In other words, the HDS performance of the  $\text{O}_2$ -passivated and then reduced  $\text{Ni}_2\text{P}/\text{MCM-41}$

was improved by the incorporation of sulfur in the catalyst. The formed phosphosulfide layer of  $\text{Ni}_2\text{P}$  seems to be more active than the clean  $\text{Ni}_2\text{P}$  surface in the HDS reaction. This observation may account for the gradual increase of HDS activity of metal phosphides in the first few hours of HDS reaction [3,4,13,22].

The TEM images in Fig. 4 show that a smooth surface was formed after  $\text{H}_2\text{S}$  passivation, whereas a rough one was obtained



**Fig. 11.** Performance of H<sub>2</sub>S-passivated Ni<sub>2</sub>P/MCM-41 in consecutive HDS, HDO, and HDS.

for the O<sub>2</sub>-passivated Ni<sub>2</sub>P, implying that a milder surface reconstruction takes place in H<sub>2</sub>S passivation. In H<sub>2</sub>S passivation, H<sub>2</sub>S dissociates readily on the surface of Ni<sub>2</sub>P [23].

XPS characterization revealed that two sulfur species were presented on the surface of H<sub>2</sub>S-passivated Ni<sub>2</sub>P/MCM-41. The species with binding energy of 163.7 eV was attributed to a polysulfide species [20,21] rather than to S<sup>2-</sup>, such as in NiS or adsorbed H<sub>2</sub>S, or (a much less extent) to S<sub>2</sub><sup>2-</sup>, because the S(2p) binding energies of S<sup>2-</sup> and S<sub>2</sub><sup>2-</sup> are located at 161.7 ± 0.3 and 162.5 ± 0.3 eV respectively [20]. It is more likely that the dissociated sulfur atoms are bonded to the surface sites of Ni<sub>2</sub>P, probably leading to the formation of phosphosulfides. The S(2p) binding energy peak at 169.9 eV suggests that sulfur species on the surface of the passivation layer were oxidized to sulfates or sulfonic species in air. Despite the partial oxidation, the H<sub>2</sub>S-passivated Ni<sub>2</sub>P/MCM-41 catalyst was fairly stable. The passivated catalysts showed equivalent HDS activity to the freshly passivated catalyst after being kept in air for 30–150 days (Fig. 5). The N(1s) signal for the NH<sub>3</sub>-passivated Ni<sub>2</sub>P/MCM-41 (Fig. 8d) showed only one main component with binding energy centered at 399.9 eV due to cationic nitrogen [24], suggesting that NH<sub>3</sub> was strongly adsorbed on the surface of Ni<sub>2</sub>P/MCM-41. These strongly adsorbed NH<sub>3</sub> species may act as a base or electronic donor, and thus transform the surface Ni and P species to an electron-rich state (Figs. 8a and 8b).

**Table 1**

Sulfur and nitrogen contents of Ni<sub>2</sub>P/MCM-41 after passivation and hydrotreating reaction.

Entry	Post-treatment	HDS/HDO/HDN	S (wt%)	N (wt%)	Ni/P/S ratio	(n <sub>S</sub> + n <sub>N</sub> ) <sup>a</sup> (mmol g <sup>-1</sup> )
1	H <sub>2</sub> S passivation	Blank	0.661	–	1/0.5/0.078	–
2	<i>In situ</i> reduction	HDS	0.597	–	1/0.5/0.072	–
3	H <sub>2</sub> S passivation	HDS	0.689	–	1/0.5/0.083	–
4	30 d after H <sub>2</sub> S passivation	HDS	0.694	–	1/0.5/0.084	–
5	O <sub>2</sub> passivation–H <sub>2</sub> reduction	HDS	0.613	–	1/0.5/0.074	–
6	O <sub>2</sub> passivation	HDS	0.391	–	1/0.5/0.047	–
7	NH <sub>3</sub> passivation	HDS	0.288	–	1/0.5/0.035	–
8	NH <sub>3</sub> passivation–H <sub>2</sub> reduction	HDS	0.361	–	1/0.5/0.043	–
9	H <sub>2</sub> S passivation	HDS–HDO	0.346	–	1/0.5/0.042	–
10	H <sub>2</sub> S passivation	HDS–HDN	0.346	0.418	1/0.5/0.042	0.407
11	H <sub>2</sub> S passivation	HDS–HDO–HDS	0.482	–	1/0.5/0.058	–
12	H <sub>2</sub> S passivation	HDS–HDN–HDS	0.656	0.339	1/0.5/0.079	0.447
13	H <sub>2</sub> S passivation	HDN–HDS	0.543	0.371	1/0.5/0.066	0.435
14	H <sub>2</sub> S passivation	HDN	0.522	0.422	1/0.5/0.063	0.465
15	H <sub>2</sub> S passivation	HDO–HDS	0.45	–	1/0.5/0.054	–

Reaction conditions for HDS, HDN, and HDO: 300 °C, WHSV 24<sup>-1</sup>, 4.0 MPa. Feed: 0.8 wt% DBT, 1.0 wt% quinoline, 1.0 wt% phenol.

<sup>a</sup> The total molar content of sulfur and nitrogen per gram of catalyst.

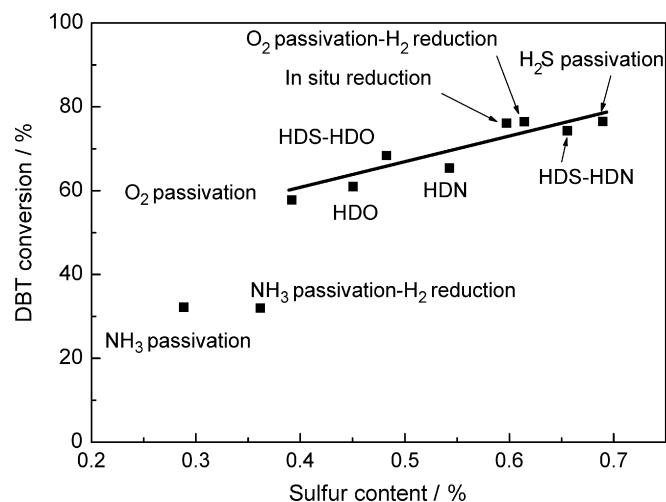


**Fig. 12.** DBT conversion as a function of sulfur content on Ni<sub>2</sub>P/MCM-41 after HDS reaction (24 h).

After passivation by H<sub>2</sub>S, O<sub>2</sub>, and NH<sub>3</sub>, the CO uptake of Ni<sub>2</sub>P/MCM-41 became zero, indicating that the “active sites”, which are sensitive to O<sub>2</sub>, were covered or replaced by H<sub>2</sub>S, O<sub>2</sub>, and NH<sub>3</sub>. If these sites are occupied by sulfur species, a phosphosulfide phase may form in the passivation step. Hence, it is not necessary to re-reduce the catalyst prior to the HDS reaction. It is interesting to note that a steady state was achieved much faster for the H<sub>2</sub>S-passivated Ni<sub>2</sub>P/MCM-41 than for the O<sub>2</sub>-passivated Ni<sub>2</sub>P/MCM-41 in the HDS of DBT.

TPD in He of the H<sub>2</sub>S-passivated Ni<sub>2</sub>P/MCM-41 revealed that H<sub>2</sub>S passivation may lead to the adsorption of H<sub>2</sub>S and dissociation of H<sub>2</sub>S to form weakly-coordinated bonds on the surface of Ni<sub>2</sub>P. According to the FTIR spectrum of pyridine adsorbed on the Ni<sub>2</sub>P/MCM-41 catalysts passivated by different gases, Brønsted acid sites were generated after H<sub>2</sub>S passivation whereas no distinct Brønsted acid sites were observed on the O<sub>2</sub>- or NH<sub>3</sub>-passivated Ni<sub>2</sub>P/MCM-41. The Brønsted acid sites might be associated with –SH groups generated by dissociation of H<sub>2</sub>S on the surface. These weakly bond species keep the Ni<sub>2</sub>P particles stable in air. The TPD profile of the spent Ni<sub>2</sub>P/MCM-41 indicates that there are mainly two kinds of sulfur species retained on the surface of Ni<sub>2</sub>P after the HDS reaction. The peaks below 400 °C likely correspond to adsorbed H<sub>2</sub>S and weakly bonded sulfur species, whereas the peaks above 600 °C might result from those sulfur atoms which are incorporated in the crystal structure. The appearance of the



high temperature peaks after the HDS reaction suggests that further sulfur-associated surface reconstruction occurs in the course of HDS. This surface reconstruction may be related to the gradual increase in HDS activity in the first few hours. Wu et al. also observed two types of sulfur species, i.e. reversibly and irreversibly bonded sulfur species, in a spent MoP catalyst [4]. They proposed that the irreversibly bonded sulfur species were detrimental to HDS performance.

Sulfur, oxygen, and nitrogen are involved in hydrotreating reactions, and inevitably interact with the active sites on the surface of the catalysts. Like O<sub>2</sub> and H<sub>2</sub>S, NH<sub>3</sub> will cover the active sites on the surface of Ni<sub>2</sub>P/MCM-41 at ambient temperature and pressure, as evidenced by the CO chemisorption results. It seems that NH<sub>3</sub>, H<sub>2</sub>S, and O<sub>2</sub> cover or replace the same type of active sites in the Ni<sub>2</sub>P/MCM-41 catalysts, but NH<sub>3</sub> passivation gave rise to a dramatic decrease in HDS activity. In contrast to the O<sub>2</sub>-passivated Ni<sub>2</sub>P/MCM-41, re-reduction led only to a minor improvement in the HDS performance for the NH<sub>3</sub>-passivated catalyst (Fig. 1). Once nitrogen species occupy the active sites, they can hardly be removed by re-reduction or be replaced by sulfur species in the course of the HDS reactions. On the other hand, if nitrogen species are introduced in the H<sub>2</sub>S-passivated Ni<sub>2</sub>P/MCM-41 by the HDN reaction (Fig. 10), the HDS activity increased slowly in the course of the HDS reaction, probably due to a gradual replacement of nitrogen species by sulfur species. If the reaction was started with HDS followed by HDN (Fig. 8), a similar trend was observed as when the reaction was changed from HDN to HDS. These observations indicate that if the active structure is well protected by H<sub>2</sub>S passivation the nitrogen species introduced by HDN are reversibly adsorbed and can be replaced by sulfur.

If the H<sub>2</sub>S-passivated Ni<sub>2</sub>P/MCM-41 is used to catalyze the HDO of phenol after HDS, the catalyst is very active and stable for 100 h in HDO, although the HDO activity did not immediately achieve a high level. When the reaction was shifted from HDO to HDS, the HDS activity recovered immediately.

The sulfur content after HDS–HDN equaled that after HDS–HDO (Table 1). This suggests that nitrogen and oxygen replace the same sulfur sites on the surface of Ni<sub>2</sub>P. These replaced sulfur atoms might be the phosphosulfide active sites. In the consecutive HDS–HDN–HDS experiment (Fig. 9), the replacement of sulfur by nitrogen was much faster than that of nitrogen by sulfur. In the case of consecutive HDS–HDO–HDS (Fig. 11), the replacement of sulfur by oxygen was dramatically slower than that of oxygen by sulfur.

The plot of the HDS performance of various Ni<sub>2</sub>P/MCM-41 catalysts against the sulfur content after HDS reaction shows that the performance is roughly correlated with the sulfur content, indicating the important role of sulfur in the Ni<sub>2</sub>P-catalyzed HDS and other hydrotreating reactions.

## 5. Conclusions

A H<sub>2</sub>S-passivated Ni<sub>2</sub>P/MCM-41 showed higher HDS activity than an O<sub>2</sub>-passivated counterpart. The H<sub>2</sub>S-passivated Ni<sub>2</sub>P/MCM-41 was stable up to 150 days. Moreover, it was not necessary to re-reduce the H<sub>2</sub>S-passivated Ni<sub>2</sub>P/MCM-41 prior to the HDS reaction. Therefore, it is concluded that H<sub>2</sub>S passivation is superior to O<sub>2</sub>

passivation in the preparation of nickel phosphide HDS catalysts. NH<sub>3</sub>-passivated Ni<sub>2</sub>P/MCM-41 exhibited a dramatically lower HDS activity than the H<sub>2</sub>S- or O<sub>2</sub>-passivated counterparts. In contrast to the O<sub>2</sub>-passivated Ni<sub>2</sub>P/MCM-41, the H<sub>2</sub> re-reduction at 500 °C only slightly improved the performance of the NH<sub>3</sub>-passivated catalyst. XPS characterization revealed that the sulfur species on the surface of the H<sub>2</sub>S-passivated Ni<sub>2</sub>P/MCM-41 were polysulfide ligands rather than S<sup>2-</sup> or S<sub>2</sub><sup>2-</sup> and the sulfur species were partially oxidized. After NH<sub>3</sub> passivation, N species were strongly bonded to the surface sites of Ni<sub>2</sub>P.

An alternating HDS–HDN–HDS investigation indicated that the replacement of sulfur by nitrogen was much faster than that of nitrogen by sulfur. In the case of consecutive HDS–HDO–HDS, the replacement of sulfur by oxygen was much slower than that of oxygen by sulfur. Ni<sub>2</sub>P/MCM-41 showed extremely high activity and stability in the HDO of phenol.

A correlation of the HDS performance with the sulfur content of the spent Ni<sub>2</sub>P/MCM-41 catalyst after HDS reaction was established: The catalyst with high sulfur content after HDS showed high HDS performance. It is therefore proposed that sulfur species or phosphosulfides serve in part as the HDS active sites.

## Acknowledgments

The authors acknowledge financial supports from the NSFC (20333030, 20503003, and 20773020), NSFC-RFBR joint project, the NCET, and the 111 Project. We thank Prof. R. Prins for helpful discussions.

## References

- [1] S. Li, J. Lee, *J. Catal.* 178 (1998) 119.
- [2] E. Furimsky, *Appl. Catal. A* 240 (2003) 1.
- [3] S.T. Oyama, X. Wang, Y.-K. Lee, K. Bando, F.G. Requejo, *J. Catal.* 210 (2002) 207.
- [4] Z. Wu, F. Sun, W. Wu, Z. Feng, C. Liang, Z. Wei, C. Li, *J. Catal.* 222 (2004) 41.
- [5] A.W. Burns, K.A. Layman, D.H. Bale, M.E. Bussell, *Appl. Catal. A* 343 (2008) 68.
- [6] S.T. Oyama, X. Wang, Y.-K. Lee, W.-J. Chun, *J. Catal.* 221 (2004) 263.
- [7] T. Kawai, K.K. Bando, Y.-K. Lee, S.T. Oyama, W.-J. Chun, K. Asakura, *J. Catal.* 241 (2006) 20.
- [8] H. Loboué, C. Guillot-Deudon, A.F. Popa, A. Lafond, B. Rebours, C. Pichon, T. Cseri, G. Berhault, C. Geantet, *Catal. Today* 130 (2008) 63.
- [9] A.E. Nelson, M. Sun, A.S.M. Junaid, *J. Catal.* 214 (2006) 180.
- [10] S. Sloboshanin, R.K. Gebhardt, J.A. Schaefer, T. Chasse, *Surf. Sci.* 431 (1999) 252.
- [11] A. Wang, T. Kabe, *Chem. Commun.* (1999) 2067.
- [12] X. Wang, P. Clark, S.T. Oyama, *J. Catal.* 208 (2002) 321.
- [13] S.J. Sawhill, D.C. Phillips, M.E. Bussell, *J. Catal.* 215 (2003) 208.
- [14] S. Yang, C. Liang, R. Prins, *J. Catal.* 241 (2006) 465.
- [15] A. Wang, L. Ruan, Y. Teng, X. Li, M. Lu, J. Ren, Y. Wang, Y. Hu, *J. Catal.* 229 (2005) 314.
- [16] J. Ren, A. Wang, X. Li, Y. Chen, H. Liu, Y. Hu, *Appl. Catal. A* 344 (2008) 175.
- [17] N.Y. Topsøe, H. Topsøe, *J. Catal.* 139 (1993) 641.
- [18] Y.-K. Lee, S.T. Oyama, *J. Catal.* 239 (2006) 376.
- [19] I.I. Abu, K.J. Smith, *J. Catal.* 241 (2006) 356.
- [20] Y. Li, R.A. van Santen, Th. Weber, *J. Solid State Chem.* 181 (2008) 3151.
- [21] J.E. Thomas, C.F. Jones, W.M. Skinner, R.St.C. Smart, *Geochim. Cosmochim. Acta* 62 (1998) 1555.
- [22] T.I. Korányi, Z. Vít, D.G. Poduval, R. Ryoo, H.S. Kim, E.J.M. Hensen, *J. Catal.* 253 (2008) 119.
- [23] P. Liu, J.A. Rodriguez, T. Asakura, J. Gomes, K. Nakamura, *J. Phys. Chem. B* 109 (2005) 4575.
- [24] C. Barthet, S.P. Armes, M.M. Chehimi, C. Bilem, M. Omastova, *Langmuir* 14 (1998) 5032.